



OPEN Intestinal microbiota improves inflammation and cognitive function in the brain of $\alpha 7$ nAChR deficient rat through the gut brain axis

Chi Cao^{2,6}, Shulin Li^{3,6}, Wencheng Wang⁴, Lei Shi², Rui Ma⁵, Bin Zhang²✉ & Jianying Tian¹✉

To investigate the role of intestinal flora and cholinergic anti-inflammatory pathways in the gut-brain axis, using oral gavage and intraperitoneal injection of methyllycaconitine (MLA). MLA was administered at a dose of 4 mg/kg for 30 days, either orally or via intraperitoneal injection. Rats were then assessed for behavioral changes, inflammatory markers, neurotransmitters, neuroreceptors, and intestinal mucosal barrier integrity. Rats receiving MLA via intraperitoneal injection exhibited significant behavioral abnormalities compared to the control and orally administered MLA groups. The levels of IL-1 β were elevated in both intestinal and hippocampal tissues, while IL-10 levels were decreased. Brain-derived neurotrophic factor (BDNF) was significantly lower in hippocampal tissues. Furthermore, $\alpha 7$ nAChR expression was reduced in hippocampal tissues, accompanied by an increase in 5-HT3A receptors. The intestinal mucosal barrier was compromised, as evidenced by reduced expression of ZO-1 and Occludin, along with increased IL-1 β and decreased IL-10 levels in the gut. Our findings suggest that oral gavage of MLA does not induce cognitive impairment in rats compared to intraperitoneal injection, possibly due to the involvement of intestinal flora in the protective effects of CAP.

Keywords Methyllycaconitine, $\alpha 7$ nAChR, Gut-brain axis, Intestinal microbiotas, Inflammation

The acetylcholine receptor (AChR) is a transmembrane protein embedded in the cell membrane that binds to the neurotransmitter acetylcholine, triggering physiological responses. AChRs are categorized into two major classes: nicotinic (nAChRs) and muscarinic (mAChRs), widely distributed in neuronal and immune cells. Neuronal AChRs are Cys-loop ion channel receptors, a family that also includes muscle-type AChRs, γ -aminobutyric acid (GABA) receptors, glycine receptors, and serotonin 5-HT3 receptors¹. In humans, nAChRs are composed of 16 subunits, including $\alpha 1$ –7, $\alpha 9$ –10, $\beta 1$ –4, γ , δ , and ϵ ². While several nAChR subtypes exist, the $\alpha 4\beta 2$ and $\alpha 7$ nAChR subtypes are predominantly expressed in the central nervous system.

Methyllycaconitine (MLA) is an alkaloid extracted from the seeds of Larkspur plants (*Delphinium barbeyi*) and has a long history of use as an insecticide against lepidopteran insect pests due to its toxicity³. The toxicity of all larkspurs is due to norditerpenoid alkaloids, which consist of two predominant types, the N-(methylsuccinimido) anthranoyllycoctonine (MSAL) type including methyllycaconitine (MLA) and the non MSAL-type including the 7,8-methylenedioxylycoctonine (MDL) type such as the alkaloid deltaline⁴.

It is an $\alpha 7$ nAChR-specific antagonist that competes with α -bungarotoxin for binding to the same receptor site. A well-established model of cognitive impairment in rats involves the intraperitoneal injection of MLA. Numerous studies have confirmed the ability of MLA-induced inflammation to produce cognitive dysfunction and behavioral changes^{5,6}.

¹School of Basic Medical Sciences, Ningxia Medical University, Yinchuan 750004, China. ²The General Hospital of Ningxia Medical University, Yinchuan 750004, China. ³The 942 Hospital of the Joint Logistics Support Force of the Chinese People's Liberation Army, Lanzhou, China. ⁴People's Hospital of Ningxia Hui Autonomous Region, Yinchuan 750002, China. ⁵The First People's Hospital of Yinchuan, Yinchuan, China. ⁶Cao Chi and Shulin Li contributed equally to this work. ✉email: zhb.1007@163.com; tenengyi1963@163.com

The brain-gut axis refers to a bidirectional regulatory system of interaction between the gut and the brain, and gut flora is now considered to be an essential regulator of brain-gut interaction. The proposed gut-brain axis provides new perspectives and ideas for studying many diseases.

Few studies have examined oral gavage MLA, and it is not known whether it can also produce a model of cognitive impairment similar to that of intraperitoneal injection. This study investigated the effects of different MLA methods on cognitive function in rats and whether gut microbes participate in the regulation of cognitive function caused by MLA.

Materials and methods

Animals

All animal experiments complied with the ARRIVE guidelines and were approved by the Animal Ethics Committee of Ningxia Medical University (Approval Number: 2020-320). All animal studies were performed following the American Veterinary Medical Association (AVMA) Guidelines for the Euthanasia of Animals (2020) guide for the Care and Use of Laboratory Animals. All methods were performed in accordance with the ARRIVE guidelines.

Twenty-seven healthy male Sprague-Dawley (SD) rats (dams, weight: 17 ± 2 g; SPF) were obtained from the Experimental Animal Center of Ningxia Medical University and randomly divided into three groups: a control group (Con), an MLA 4 mg/kg oral gavage group (MLA-O), and an MLA 4 mg/kg intraperitoneal injection group (MLA). The rats were housed in a controlled environment with a relative humidity of 45–55%, a temperature of 20–22 °C, and a 12-hour light/dark cycle. All rats had *ad libitum* access to food and water.

Reagents

The MLA configuration method is as follows: The corresponding MLA powder is weighed according to the rat's body weight, and the total volume is calculated based on 0.1 ml per 100 g of body weight. 5% of the total volume of DMSO is used to dissolve the MLA powder, and the remaining volume is mixed with the DMSO solution using corn oil.

Morris water maze test (MWM)

This experiment evaluated the learning and memory capabilities of rats using an automatic observation system to record their trajectories and assess the time and distance traveled from the starting point to a submerged platform in a circular pool, kept at a water temperature of 22 ± 2 °C⁷. A 10 cm diameter platform was placed 1–2 cm underwater and the water was dyed with liquid caramel colouring (Aipu Food Industry Co., Ltd.) to obscure the platform. During the first 4 days, a training period was conducted, in which each rat was launched from each of the 4 quadrants and allowed to swim for 1 min. If the platform could not be found, the rat was guided onto the platform and was made to wait for 1 min. On Day 5, the platform was retained to test the escape latency time. On Day 6, the platform was removed to test the cross-platform times⁸.

The novel object recognition test (NOR)

Rats were initially placed in a field for 10 min on the first day. On the second day, two identical conical objects (A and B) were introduced to the field. On the third day, one of the objects was replaced with a novel object⁹. Exploration time was recorded when the rat's nose and mouth were less than 1 cm from the object or directly touching the object¹⁰. At the end of each rat test 75% alcohol was used to eliminate the odor and to clean up the rat excreta. The time spent by the rats exploring each object was recorded using an automated system. The discrimination index (DI) was calculated as follows: $DI = [(time\ spent\ exploring\ new\ object - time\ spent\ exploring\ old\ object) / (time\ spent\ exploring\ new\ object + time\ spent\ exploring\ old\ object)] * 100\%$. The test period preference index (PI) was calculated as: $PI = time\ spent\ exploring\ new\ object / (time\ spent\ exploring\ new\ object + time\ spent\ exploring\ old\ object)$.

Sample collection

Following the completion of behavioral testing, rats were anesthetized with isoflurane (induction dose: 3%, maintenance dose: 1%). The hippocampus and gut were harvested and immediately stored at -80 °C for further analysis. At the end of the experiment, all animals were euthanized by a lethal dose of isoflurane (dose: 8%), and euthanized by cervical dislocation.

Immunofluorescence

Rat small intestine and brain tissues were sectioned into 5- μ m paraffin-embedded slices, dewaxed in xylene, rehydrated in a gradient of alcohol, and subjected to antigen retrieval in sodium citrate buffer (ZSGB Biotechnology; ZLI-9064). After cooling to room temperature, the sections were blocked with a non-specific binding blocker for 2 h and washed thoroughly in phosphate-buffered saline (PBS). Primary antibodies against ZO-1, Occludin, $\alpha 7nAChR$, 5-HT3A, and IL-1 β were applied overnight at 4 °C. Following incubation, the sections were washed in PBS, stained with a DAPI-containing anti-fluorescence quenching agent, dried, and visualized under a microscope.

Western blot (WB)

The hippocampal and small intestinal tissues of rats were placed in pre-cooled tubes containing RIPA total protein lysate and centrifuged at 12,000 rpm for 10 min, at 4 °C twice. The supernatants were collected, and protein concentrations were determined using a bicinchoninic acid kit (KeyGEN; KGP902). Protein samples were paired with 5X loading buffer and dd H₂O and then boiled at 100 °C for 5 min. Equivalent amounts of protein were boiled, proteins were separated using 10% SDS-PAGE gel, and transferred to 0.45 μ m PVDF

membranes. 5% skimmed milk was used for blocking 2 h blocking, after that the membranes were incubated with primary antibodies overnight at 4 °C, followed by HRP-coupled secondary antibodies for 1 h (KeyGEN; KGP1121). Bands were analyzed via Image J (version:1.53a) greyscale values and compared with those of β -actin or GAPDH to obtain relative expression values.

Real-time quantitative polymerase chain reaction (RT-PCR)

Total RNA was extracted from rat hippocampi using the TRIzol[®] method (Vazyme Biotech Co., Ltd.) following the manufacturer's protocol. RNA concentration and purity were assessed spectrophotometrically by measuring absorbance at 260/280 nm and 260/230 nm. cDNA was synthesized from homogenized RNA using Hiscript II reverse transcriptase under the following conditions: 50 °C for 15 min, followed by 85 °C for 5 s. Gene expression was quantified using a LightCycler 96 Real-Time PCR System (Vazyme Biotech Co., Ltd.) with SYBR Green dyes (Vazyme Biotech Co., Ltd.). PCR conditions were as follows: 30 s of predenaturation at 95 °C, followed by 40 cycles of denaturation at 95 °C for 10 s, and annealing/extension at 60 °C for 30 seconds¹¹. GAPDH was used as an internal control, and relative gene expression was calculated using the $\Delta\Delta C_q$ method. Primer sequences are listed in Table 1.

Fecal collection

The fecal samples from all nine rats were collected aseptically in sterile tubes and stored at -80 °C. DNA was extracted from these samples using the E.Z.N.A Soil DNA Kit (Omega Biotek, Norcross, GA, U.S.) and the V4-V5 region of the bacterial 16 S ribosomal RNA gene was amplified via PCR. Amplicons were purified using the AxyPrep DNA Gel Extraction Kit (Axygen Biosciences, Union City, CA, U.S.) and quantified with QuantiFluor[™]-ST (Promega, U.S.). Sequences were clustered into operational taxonomic units (OTUs) at a 97% sequence identity using mothur (furthest neighbor method) and chop seq(Majorbio). Linear discriminant analysis effect size (LEfSe) was employed to identify OTUs with significant structural differences among the sample groups.

Statistical analysis

The data were presented as means \pm standard deviations (SDs). One-way ANOVA followed by Fisher's least significant difference (LSD) test was used to compare more than two groups. Each experiment was replicated at least three times. Statistical analyses were conducted using SPSS 20.0.0 software (IBM Corp.), and a *p*-value of <0.05 was statistically significant.

Results

Effect of oral and intraperitoneal administration of MLA on body weight and behavioral changes

The oral or intraperitoneal administration of MLA did not impact body weight. To assess the effects of different MLA administration methods on cognitive function in rats, the MWM test was conducted, as illustrated in Fig. 1A. The results indicated that MLA-administered rats required significantly longer swim distances to locate the platform than the control group (Fig. 1B). This was reflected in the increased escape latency time and average swimming distance of the MLA group (Fig. 1C,D). The track figure further revealed a distinct difference in swimming patterns between the MLA and control groups. While the control group exhibited repeated exploration of the original platform location and frequent platform crossings, the MLA group primarily swam along the pool wall with minimal platform crossings (Fig. 1E). This was corroborated by the significantly reduced number of platform crossings in the MLA group. Additionally, the average swimming speed in the target quadrant was notably lower in the MLA group compared to the control and MLA-O groups (Fig. 1F,G). The novel object recognition (NOR) test was employed to evaluate learning and memory capacity. The results demonstrated a significantly lower discrimination index (DI) in the MLA group compared to the control and MLA-O groups (Fig. 1I), indicating impaired memory function. Moreover, the preference index, which represents the preference time for new objects during the familiarity period, was significantly lower in the MLA group than in the control group (Fig. 1J). H&E staining was conducted to assess the morphological changes observed in the neurons of the CA3 region of the hippocampus tissue samples from the mice (Fig. 1K). In the control group, the neurons were arranged in a neat and orderly manner, exhibiting a regular morphology, minimal anisotropy, and a clear hierarchical structure. Their nuclei were rounded, light in color, and easily visible. In contrast, the MLA-O group demonstrated a more clearly arranged neuronal structure, with a generally regular morphology, although a few individual neurons displayed vacuoles. However, the MLA group exhibited a significant reduction in the number

Gene	Forward primer (5'-3')	Reverse primer (5'-3')
BDNF	GTGTGACAGTATTAGCGAGTGGG	ACGATTGGGTAGTTCCGGCATT
IL-1 β	GAACAACAAAATGCCTCGTGC	GACAAACCGCTTTTCCATCTTCT
IL-10	CCTGGCTCAGCACTGCTATGT	TTGGCAACCCAAGTAACCCTTA
CHRNA7	GAAGTTTGGGTCCTGGTCCTATG	GGTGACATCTGGGTATGGCTCT
5-HT3AR	TCAATGAGTTTGTGGACGTGGG	ATAGATGTCAAGGCTACAGGCGG
ZO-1	GAGTTTGACAGTGGAGTCG	AGCTGAAGGACTCACAGGAA
Occludin	TCGGTACAGCAGCAACGATAA	CTGTCGTGTAGTCGGTTTCATA

Table 1. Primer sequence.

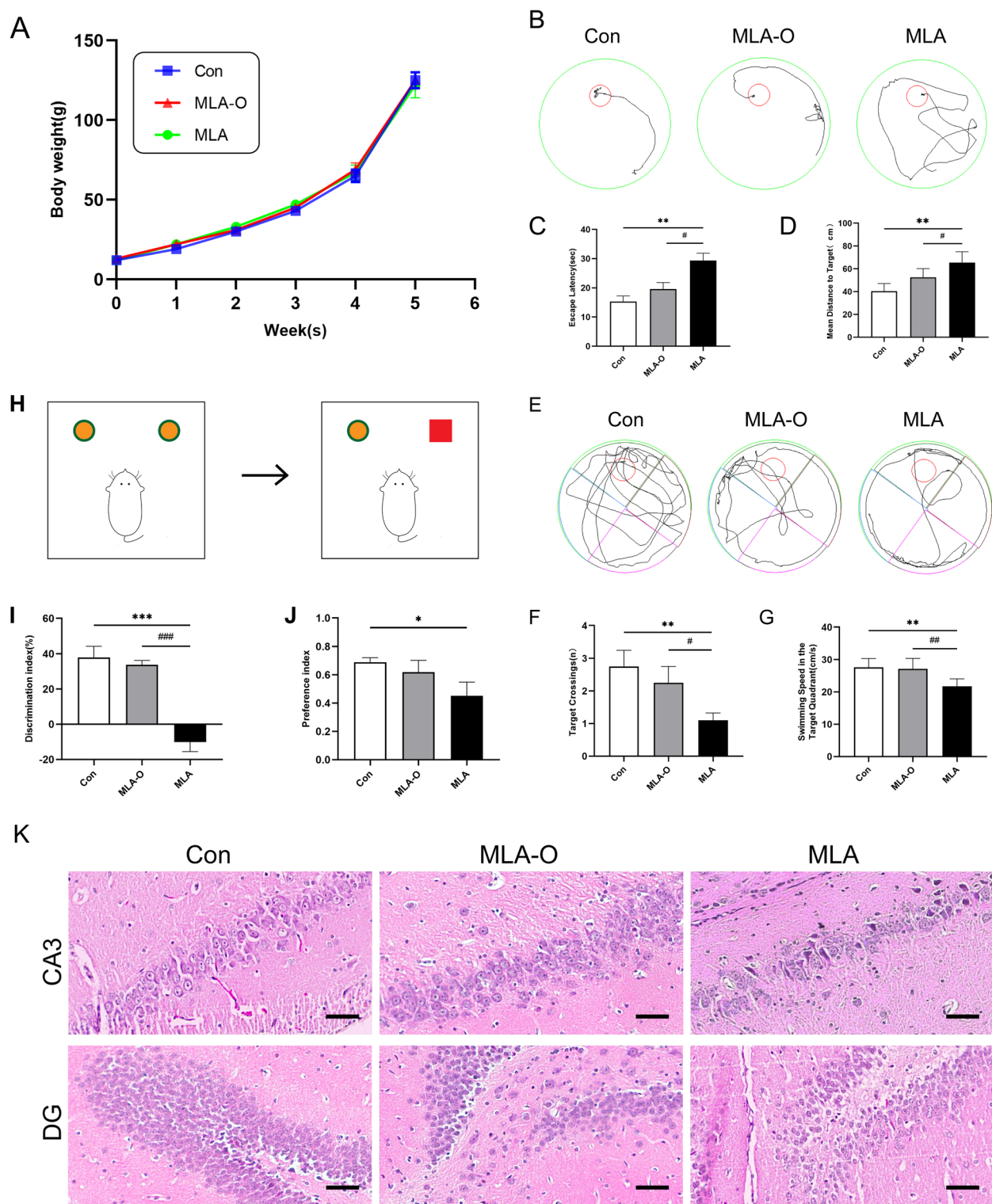


Fig. 1. Changes in the body weight and behavior of rats after MLA intervention through different pathways. **(A)** Effects of MLA on body weight in rats. **(B–G)** MWM test results. **(H–J)** NOR test results. **(K)** H&E staining of hippocampal neurons in the rat brain. Magnification 400 ×, scale bar = 50 μm.

of neurons, accompanied by disordered arrangement, increased anisotropy, and nuclear shrinkage. Furthermore, some nuclei were absent or exhibited disrupted nucleoli. Concomitantly, the cytoplasm appeared turbid, with ill-defined strata and a diminished number of layers. Furthermore, an expansion of the intercellular spaces was observed. In the DG area, the neurons of the control group were regularly arranged and orderly, with a regular morphology and clear layers. The MLA-O group also displayed a neat arrangement, with a few cells showing

vacuoles. However, the MLA group demonstrated disordered neuronal arrangement, unclear layers, increased intercellular spaces, a higher frequency of cells with nuclear fixation, and an abundance of vacuoles.

MLA-induced changes in hippocampal neurotransmitter systems

Next, the expression of $\alpha 7$ nAChR in the DG region of the hippocampus and the CA3 region was assessed (Fig. 2A, B). Compared with the Con group and the MLA-O group, the number of $\alpha 7$ nAChR positive cells was significantly lower in the MLA-O group (Fig. 2C). The number of $\alpha 7$ nAChR-positive cells was significantly lower in the MLA group than in the Con and MLA-O groups (Fig. 2D). The expression of $\alpha 7$ nAChR, BDNF, and IL-1 β in the MLA group was significantly downregulated, and the expression of 5-HT3AR and IL-1 β was significantly

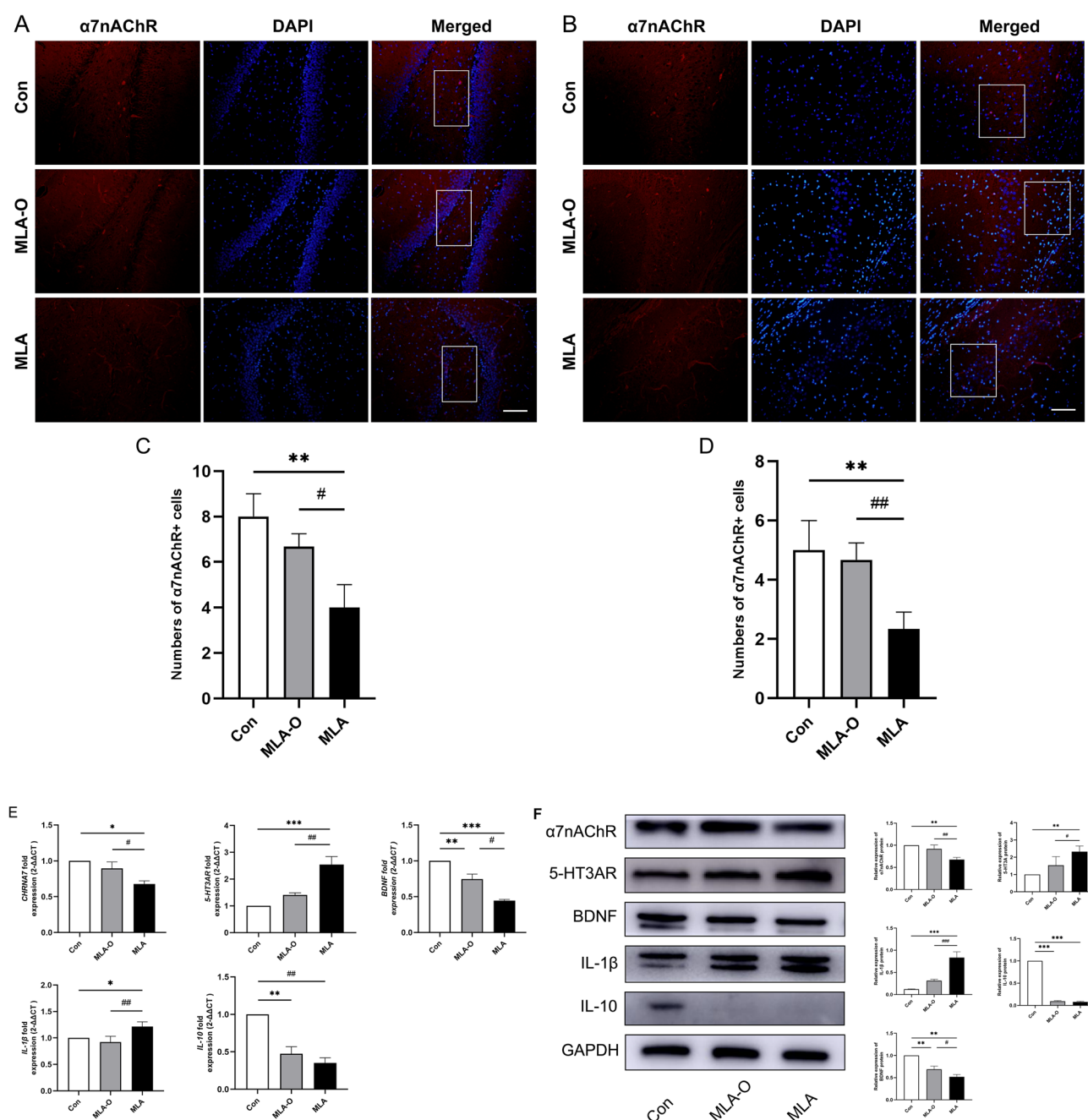


Fig. 2. The effects of different administration methods of MLA on neurotransmitters and inflammatory factors in the brain. **(A)** The number of $\alpha 7$ nAChR positive cells in the DG region of the hippocampus. **(B)** The number of $\alpha 7$ nAChR positive cells in the CA3 region of the hippocampus. Magnification 400 \times , Scale bar = 50 μ m. **(C)** The number of $\alpha 7$ nAChR positive cells in the DG region. **(D)** The number of $\alpha 7$ nAChR positive cells in the CA3 region. **(E)** Relative expression of mRNA of CHRNA7, 5-HT3AR, BDNF, IL-1 β , and IL-10 in hippocampal tissue of rats. **(F)** The protein expression levels of $\alpha 7$ nAChR, 5-HT3AR, BDNF, IL-1 β , and IL-10 in hippocampal tissues.

upregulated (Fig. 2E). Next, we examined the protein expression level of $\alpha 7$ nAChR, BDNF, IL-10, 5-HT3AR, and IL-1 β . The results showed that the expression of $\alpha 7$ nAChR, BDNF, and IL-10 was significantly lower in the MLA group, and the expression of 5-HT3AR and IL-1 β was significantly increased in the MLA group (Fig. 2F).

Expression of the small intestinal mucosal barrier and inflammatory factors

The expression of the small intestinal mucosal barrier and inflammatory factors was assessed in the MLA group, which exhibited significantly lower numbers of ZO-1 and Occludin-positive cells than the Con group (Fig. 3A–C).

Additionally, the MLA group displayed a significantly lower number of IL-10 positive cells than both the Con and MLA-O groups (Fig. 3D,E), indicating a compromised immune response. Conversely, the number of IL-1 β -positive cells was significantly higher in the MLA group than in the Con and MLA-O groups (Fig. 3F,G), suggesting heightened inflammation. To further investigate the expression of inflammatory factors, Western blotting was employed to measure protein levels. The results revealed significantly lower protein expression of IL-10 in the MLA group (Fig. 3J,K) and significantly higher protein expression of IL-1 β in the MLA group (Fig. 3H,I), corroborating the immunohistochemical findings and highlighting the dysregulated inflammatory status in the MLA group.

Changes in intestinal flora diversity in rats after different modes of MLA administration

To assess compositional disparities among the three rat colony groups, we employed beta diversity analysis. Principal coordinate analysis (PCoA) of amplicon sequence variants (ASVs) demonstrated distinct clustering patterns corresponding to the three groups at the genus level, as illustrated in Fig. 4A. To isolate within-group variations while controlling for between-group effects, we utilized the non-metric multidimensional scaling (NMDS) model. The NMDS plots presented in Fig. 4B,C revealed significant differences among the groups, suggesting that each colony harbored a unique bacterial community.

To assess the differential flora's contribution to variance and relative abundance in each sample, we conducted a linear discriminant analysis (LDA) coupled with effect size measurement (LefSe) analysis. The LefSe analysis identified three distinct groups, with the MLA-O group exhibiting the highest LDA scores at the genus level. Specifically, *Butyrivoccus*, *Lachnospiraceae_NK4A136_group*, *Peptococcus*, *UCG_010*, *Acetatifactor*, *Bacteroides*, and *Clostridium_innocuum_group* demonstrated the highest abundance within the Con group. When examining the two LefSe groups, the MLA-O group exhibited the highest LDA scores for *UCG_009* ($P=0.049$), *Anaeroplasma*, *Butyrivoccus*, *Acetatifactor*, *Intestinimonas*, and *Peptococcus*. Conversely, the

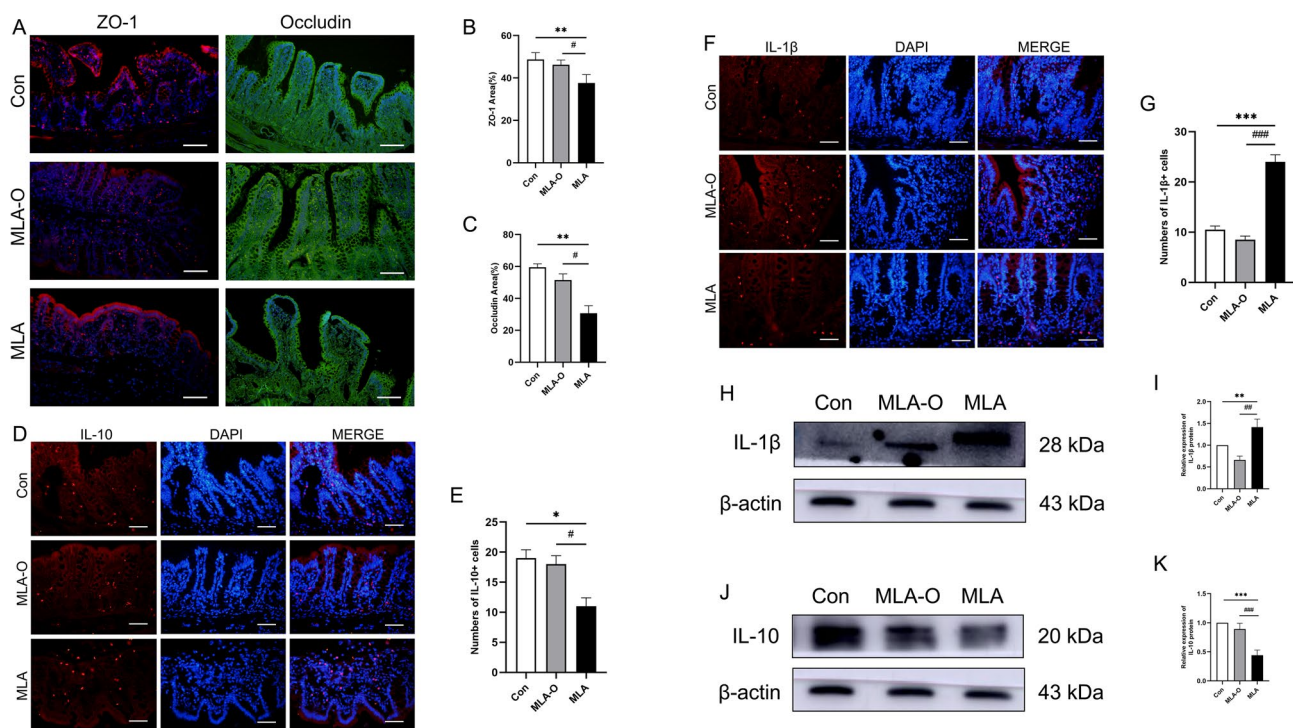


Fig. 3. Changes in intestinal mucosal function and inflammation. **(A)** ZO-1 and Occludin expression in the rat intestine. Magnification 400 \times ; scale bar = 50 μ m. **(B)** Positive expression of ZO-1. **(C)** Positive expression of Occludin. **(D)** The number of IL-10-positive cells in the intestine. **(E)** Positive expression of IL-10. Magnification 400 \times ; scale bar = 50 μ m. **(F)** The number of IL-1 β positive cells in the intestine. Magnification 400 \times , Scale bar = 50 μ m. **(G)** Positive expression of IL-10. **(H)** Protein-expression blotted strips of IL-1 β **(I)**. The relative expression of IL-1 β . **(J)** Protein-expression blotted strips of IL-10. **(K)** The relative expression of IL-10.

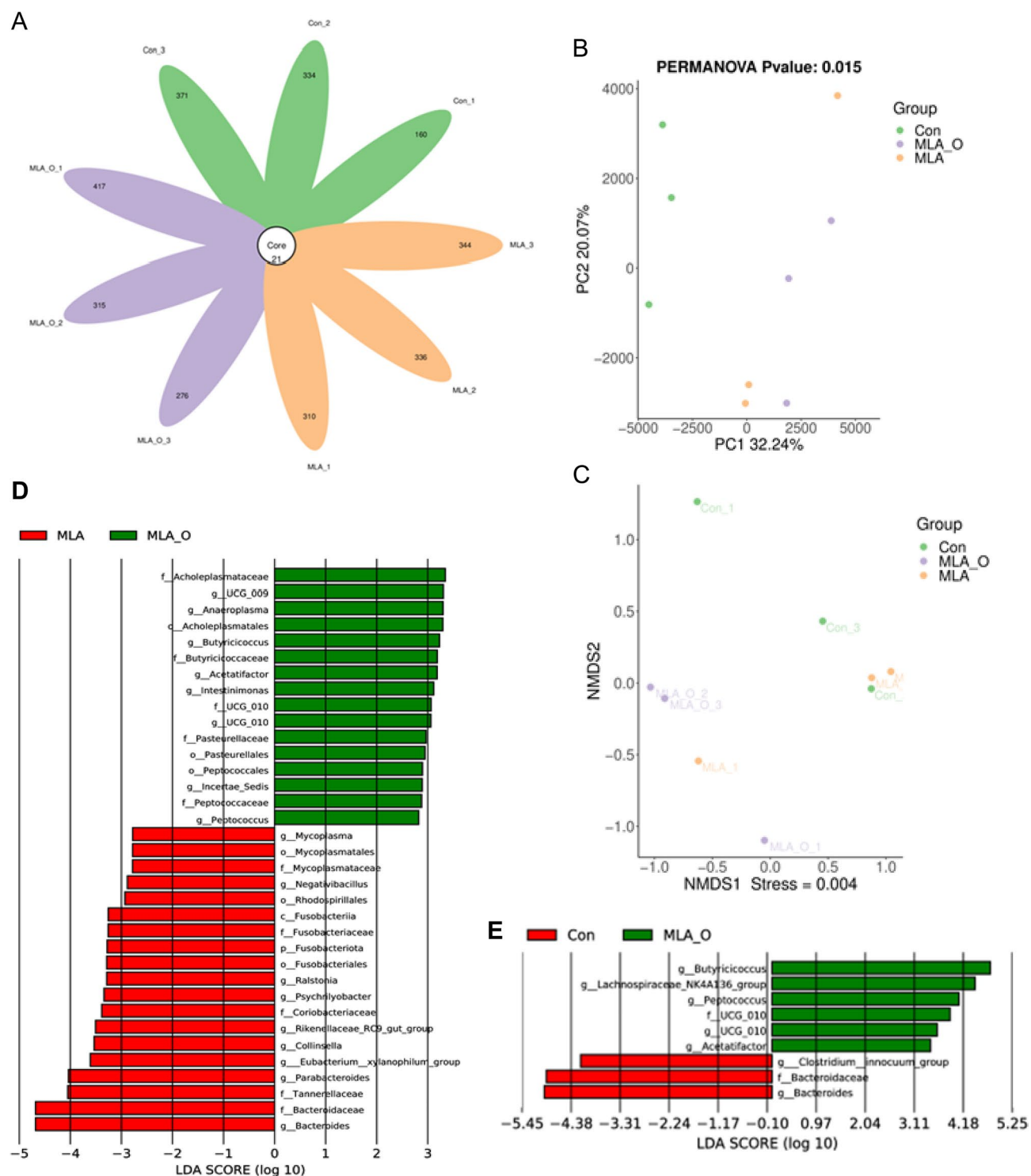


Fig. 4. β -diversity analysis of different groups. (A) Venn diagram at the OTU level. (B) PCoA based on unweighted UniFrac distance. (C) Unweighted UniFrac NMDS plots of each sample based on the abundances of the genera. LefSe analysis among groups. (D) LefSe analysis of the bacteria in the MLA-O and MLA groups. (E) Histogram of LDA scores for differentially abundant genera between the control and miscarriage groups.

MLA group displayed higher LDA scores for *Bacteroides*, *Parabacteroides*, *Eubacterium__xylanophilum_group*, and *Collinsella*. These findings, as illustrated in Fig. 4D, E, provide valuable insights into the differential flora's impact on the overall variance and relative abundance within the samples.

Flora composition changes

The bar plot illustrates that there were no substantial disparities between the groups at the phylum level. Firmicutes were the predominant phylum in the MLA group, while Proteobacteria were most prevalent in the MLA-O group. Fusobacteriota exhibited significant differences in the MLA group compared to both the Con and MLA-O groups. The absence of a graph for the MLA group at the phylum level is attributed to the lack of appreciable changes in bacterial abundance (Fig. 5A). The heatmap likewise demonstrated similar outcomes (Fig. 5B). The Wilcoxon test revealed that, compared to the Con group, the MLA group exhibited significantly higher relative abundance values of *Deferribacterota* and significantly lower relative abundance values of *Verrucomicrobiota*. In comparison to the MLA-O group, the relative abundance of Fusobacteriota was notably higher in the MLA group (Fig. 5C,D). To further elucidate the composition of the intestinal flora in the three groups of rats, we delved into the intestinal microorganisms at the genus level. *Muribaculaceae*, *Bacteroides*, *Alloprevotella*, and *Lactobacillus* were the groups with the highest proportions at the genus level. The abundance of *Muribaculaceae* was highest among the groups, yet it did not differ significantly from *Alloprevotella* or *Lactobacillus* in any of the three groups. In the Con group, the abundance of *Bacteroides* was significantly greater than that in the MLA-O and MLA groups. Besides, the abundance of *Bacteroides* was significantly lower in the MLA-O group than in the MLA group.

The genus-level analysis revealed a significant reduction in *Parabacteroides* abundance in the MLA-O group compared to the Con and MLA groups, as evidenced by Fig. 5E and the accompanying heatmap in Fig. 5F. Further comparisons between the Con and MLA-O groups highlighted significantly lower abundances of *Parabacteroides*, *Bacteroides*, and UCG_009 in the MLA-O group (Fig. 5G). Within the MLA group, the abundance of *[Clostridium]_innocuum_group* was found to be significantly lower than in the Con group, while the *Lachnospiraceae_NK4A136_group* and *Bifidobacterium* exhibited significantly higher abundances (Fig. 5H). When comparing the MLA group to the Con group, the abundances of *Bacteroides*, *Parabacteroides*, *Rikenellaceae_RC9_gut_group*, and *Psychrobacter* were significantly lower. Conversely, the MLA group demonstrated a slight increase in *Bacteroides*, *Alloprevotella*, and *Clostridioides* abundances compared to the Con group, although these differences were not statistically significant (Fig. 5I).

Discussion

The $\alpha 7$ nAChR plays a crucial role in the cholinergic anti-inflammatory pathway (CAP), exerting anti-inflammatory effects in organisms^{12,13}, protects cholinergic neurons and enhances cognitive function in animals¹⁴. Moreover, the anti-inflammatory properties of the $\alpha 7$ nAChR contribute to its neuroprotective effects¹⁵. It has been reported that $\alpha 7$ nAChR is directly involved in hippocampal long-term potentiation (LTP), a cellular mechanism underlying cognitive function¹³. Previous studies have clearly shown that the knockout of $\alpha 7$ nAChR results in cognitive impairment in rats, and that it affects the levels of inflammatory factors in the gut and brain through the gut-brain axis. Therefore, our research intervenes in rats through different pathways using MLA to investigate whether gut microbiota are involved in the process by which $\alpha 7$ nAChR affects cognitive function.

Previous studies on larkspur extract compared the toxic responses among sheep, rats, mice, and hamsters. The results indicated that sheep were the most susceptible to toxicity by subcutaneous injection of larkspur extract with decreasing susceptibility in hamsters, mice and rats. In contrast, the susceptibility of rats, mice, and hamsters was found to be similar to that of sheep¹⁶. The mean LD50 for subcutaneous injection of a single extract in mice, hamsters and rats was not different between mice and hamsters, but the LD50 for rats was about 1.6 times higher than that for mice and hamsters⁷. The LD50 for the oral dose was about 2.8 times greater than that for the subcutaneous dose in the rat. The pharmacokinetic study of MLA showed that the maximum concentration of MLA in the brain was about 5% of that in plasma. A study on different administration methods of MLA in rats showed that plasma levels of MLA following oral(p.o.) and intraperitoneal(i.p.) delivery displayed typical distribution and linear elimination kinetics, yielding half-lives of 408 ± 25 min and 37 ± 4 min, respectively. The AUC (Area Under the Curve) of MLA following p.o. and i.p. administration was 244 and 618 ng·h/ml¹⁷. Although the AUC following i.p. injection is the highest, the $t_{1/2}$ following p.o. administration is the longest. This indicates that after i.p. injection, MLA can quickly reach peak plasma concentration in the body, but the duration of retention is shorter.

There are significant differences in the cognitive outcomes of rats between p.o. and i.p., which may be partly due to the differing absorption and bioavailability rates of MLA via these two administration routes. Literature indicates that the bioavailability of MLA in rats administered orally by gavage is approximately 17%, whereas i.p. achieves about 59%²¹. This substantial difference in bioavailability means that the dose of MLA administered orally that can produce systemic effects is relatively low. In contrast, i.p. bypasses gastrointestinal absorption and avoids hepatic metabolism, allowing nearly all MLA to enter the bloodstream and rapidly act on the brain. The differences in the AUC results between the two methods are consistent with these bioavailability findings; the significantly higher AUC following i.p. partly explains the observed notable differences in cognitive function. However, our study also has limitations. We did not measure MLA concentrations in the brains of rats in each group, so we lack specific comparative data. This aspect will be addressed in our future research.

The effects of different methods of MLA administration on the cognitive function of rats were investigated through behavioral tests and histological analysis. Our findings revealed that intraperitoneal MLA administration led to a pronounced elevation in inflammation within both the brain and the gut. Rats exposed to MLA exhibited impaired performance in the MWM and NOR tests, suggesting cognitive deficits. Histological

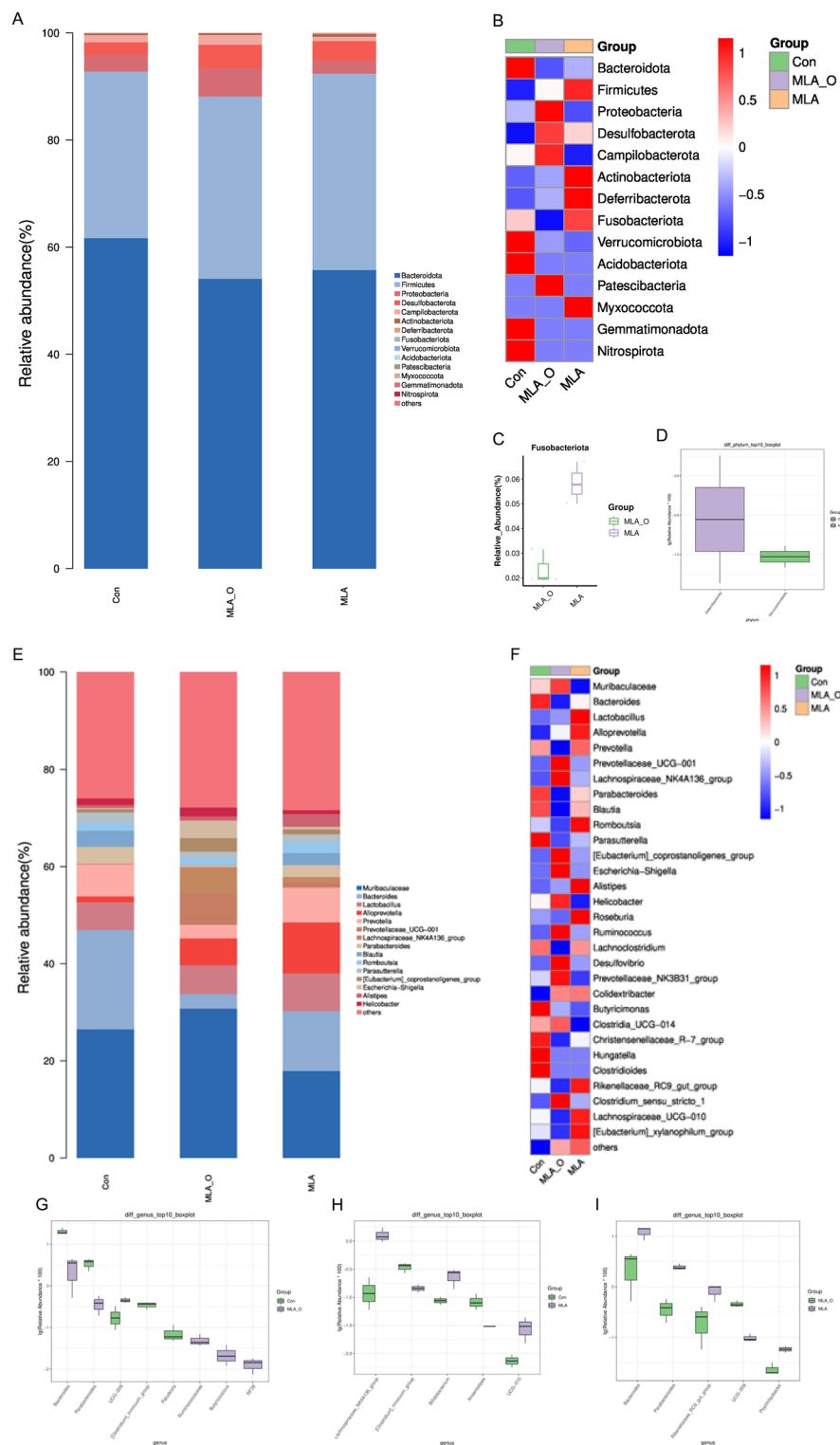


Fig. 5. Phylum- and genus-level shifts in microbiota composition. **(A)** The bar plots indicate the mean relative abundance of the top 15 phyla in the Con, MLA-O, and MLA groups. Wilcoxon analysis between the two groups. **(B)** Heatmap of the three groups of bacteria. **(C)** Comparison of differential flora between the MLA and MLA-O groups. **(D)** Comparison of differential flora between the Con and MLA groups. The result of the genus-level flora analysis. **(E)** The bar plot indicates the mean relative abundance of the top 15 genera in the Con, MLA-O, and MLA groups. Wilcoxon analysis between the two groups. **(F)** Heat map of three groups of bacteria. **(G)** Comparison of differential flora between the Con and MLA-O groups. **(H)** Comparison of differential flora between the Con and MLA groups. **(I)** Comparison of differential flora between the MLA and MLA-O groups.

examination revealed significant alterations in the hippocampus of MLA-treated rats. Given the hippocampus' crucial role in memory, cognition, and learning, these structural changes likely underlie the observed behavioral impairments. H&E staining confirmed MLA's detrimental effects on hippocampal neurons, corroborating the behavioral findings. In the hippocampus, BDNF mediates learning in novel object recognition tasks and attenuates the inflammatory damage caused by IL-1 β and TNF- α via the NF-KB pathway. The significantly lower hippocampal BDNF expression in the MLA group was closely associated with increased inflammation. We hypothesized that structural changes in hippocampal neurons may lead to functional alterations in brain receptors, particularly the α 7nAChR, pivotal in regulating cognitive function, neurotransmitter release, and neuronal protection¹⁸. Compared to the control and MLA-O groups, the MLA group exhibited significantly lower α 7nAChR expression, aligning with the MWM and NOR test results. This suggests that MLA antagonizes α 7nAChR function, contributing to the observed cognitive deficits.

In the normal gut, 5-HT functions synergistically to regulate various intestinal functions, including epithelial barrier function, fluid and electrolyte transport, mucin secretion, and motility¹⁹. 5-HT also acts as an agonist of 5-HT3AR and an antagonist of α 7nAChR²⁰. Owing to the high degree of structural similarity between α 7nAChR and 5-HTR, most α 7nAChR agonists also act as 5-HT3 antagonists²¹, such as nicotine¹³. Our findings revealed a negative correlation between 5-HT3AR expression in the brain and α 7nAChR activity, consistent with previous research. Intestinal flora metabolites, such as short-chain fatty acids (SCFAs), promote increased colonic 5-HT, enhance colonic contraction, and accelerate colonic transport¹⁰. Additionally, the intestinal flora stimulates mononuclear macrophages and mast cells to release 5-HT and alter the levels of IL-10, IL-6, and IL-1 β ¹⁷. We hypothesized that in the MLA group, the altered inflammation caused by MLA was not modulated by the intestinal flora, leading to a decrease in α 7nAChR and an increase in 5-HT3R in the brain. In contrast, the MLA-O group, with the involvement of the intestinal flora, experienced a modulated inflammatory response in the intestine, allowing normal 5-HT secretion and maintaining inflammation levels. Despite the observed inflammatory effects on the intestine, body weight remained relatively unchanged across all groups. This suggests that the intestinal inflammation induced by MLA did not substantially interfere with the metabolic processes of the rats, thereby preventing significant alterations in body weight.

The intestinal mucosal barrier primarily consists of epithelial cells, villi, and mechanical structures composed of tight junctions between cells and microbial barriers. The mucus secreted by intestinal microorganisms is a vital part of the intestinal barrier, maintaining a relatively stable dynamic barrier within the intestinal wall mucus layer and playing a role in reducing intestinal inflammation and enterogenic infection¹⁸. We investigated alterations in the intestinal mucosal barrier. Occludin is a crucial structural protein that attaches to adjacent epithelial cells, forming a barrier within the paracellular space at the apical portion of the cell²². ZO-1 is another important component of tight junctions, connecting Occludin to the actin cytoskeleton within intestinal epithelial cells²³. Immunofluorescence results revealed that the intestinal mucosal barrier was significantly compromised by intraperitoneal injection. This finding aligns with the results of the flora analysis. We hypothesized that without the involvement of the intestinal flora, inflammation in the intestine impaired the barrier function of the intestinal mucosa. This led to metabolites penetrating outside the intestine through the compromised mucosal barrier, causing a series of inflammatory reactions that eventually accumulated, resulting in damaging effects on the brain. The loss of α 7nAChR function, the inability of the CAP pathway to effectively combat inflammation, and the failure of bacterial flora to effectively regulate inflammation contributed to changes in the intestinal barrier, facilitating the transfer of inflammation from the gut to the brain. This finding is similar to previous studies on the effects of nicotine on behavior after oral administration²⁴. Our results were consistent with alterations in Occludin and ZO-1 in the gut observed after inflammatory insults, including sepsis, inflammatory bowel disease, and severe injury²⁵. Other studies using oral gavage and intraperitoneal injections to investigate intestinal mucosal function and flora have confirmed the close relationship between changes in intestinal mucosal barrier function and intestinal flora²⁶.

Significant differences were observed in the composition of the intestinal flora among the groups. At the phylum level, Bacteroidota and Firmicutes were the most abundant, but there were no significant differences among the groups, aligning with previous findings. In the MLA group, the abundance of Verrucomicrobiota and Fusobacteriota increased significantly, while the abundance of Deferribacta decreased significantly. These results were consistent with previous studies. Qi et al. found that Deferribacta was the most abundant phylum in the young flora, consistent with our findings²⁷. We hypothesized that the MLA-O group maintains a favorable microenvironment in the gut by regulating inflammation, allowing the flora to survive normally. At the genus level, bar plot analysis revealed that Muribaculaceae and Bacteroides had the highest abundance. Bacteroides is a common gram-negative beneficial bacterium in the gut. Muribaculaceae is a universal beneficial bacterium, positively correlated with glutamate. Our findings indicate that oral gavage and intraperitoneal injection differentially affect Bacteroides, with oral gavage having a more pronounced effect. The combined abundance of Bacteroides and Muribaculaceae suggests a significant impact of MLA on the intestinal flora. Lachnospiraceae_NK4A136_group, a primary producer of butyric acid, is a crucial nutrient for goblet cells, which can enhance intestinal mucosal barrier function¹⁶, regulate intestinal inflammation²⁸, and contribute to a healthy intestinal environment²⁹, indicating that MLA-induced inflammation stimulates Lachnospiraceae_NK4A136_group. However, MLA does not directly affect the intestinal flora through oral gavage, leading to less-protected intestinal barrier function. Lachnospiraceae_NK4A136_group was negatively correlated with proinflammatory factors and 5-HT, and positively correlated with BDNF. The decreased intestinal barrier function in the MLA group indicates that intraperitoneal injection of MLA promotes the Lachnospiraceae_NK4A136_group to maintain normal intestinal barrier function, although these regulatory effects were not overtly apparent. Wilcoxon analysis identified Bacteroides, Parabacteroides, and Rikenellaceae_RC9_gut_group as the most abundant bacteria in the MLA group, which are typical components of the intestinal flora. Studies have shown that Parabacteroides are positively correlated with IL-10 and can regulate inflammation and maintain intestinal homeostasis. The lowest

abundance of Parabacteroides in the MLA-O group suggests that the oral group's flora was directly affected by MLA, sacrificing these beneficial bacteria to combat inflammation. The Rikenellaceae_RC9_gut_group is associated with oxidative stress and proinflammatory factors⁷ and was significantly decreased in the MLA-O group, indicating a more pronounced effect of MLA on the intestinal flora in the oral gavage group. LEfSe results aligned with the aforementioned findings. In the MLA-O group, the highest abundance of Butyricococcus was detected, significantly different from the intraperitoneal injection group, suggesting a direct effect of MLA on the flora through oral gavage, consistent with previous results. Butyricococcus produces butyric acid, alleviates inflammation through G protein-coupled receptors, regulates the intestine³⁰, and suppresses NF- κ B to alleviate inflammation. These effects are closely related to anti-inflammatory properties, indicating that the intestinal inflammation caused by oral gavage of MLA is suppressed by the regulation of intestinal microorganisms. The study found that the brain-gut-microbiota axis plays an important role in faecal bacteria transplantation in alpha7 knockout mice produced a depressive-like phenotype³¹. This is similar to our research.

Conclusions

Overall, our findings suggest that the intestinal flora can regulate inflammation in the gut and brain induced by MLA through the gut-brain axis, thereby safeguarding the cognitive function of rats. This provides a novel perspective for the treatment of brain diseases stemming from intestinal inflammation in the future. The efficacy of oral gavage administration in reducing intracerebral inflammation may be attributed to the modulatory effects of gut microbes via the gut-brain axis.

Data availability

The datasets used and/or analyzed during the current study are available from the corresponding author upon reasonable request.

Received: 5 December 2024; Accepted: 14 May 2025

Published online: 26 May 2025

References

- Arias, H. R. Marine toxins targeting ion channels. *Mar. Drugs*. **4**, 37–69 (2006).
- Jones, A. K., Elgar, G. & Sattelle, D. B. The nicotinic acetylcholine receptor gene family of the pufferfish, *Fugu rubripes* \star . *Genomics* **82**, 441–451 (2003).
- Hooda, N. & Damani, O. A system for optimal design of pressure constrained branched piped water networks. *Procedia Eng.* **186**, 349–356 (2017).
- Olsen, J. D. & Sisson, D. V. Toxicity of extracts of tall Larkspur (*Delphinium barbeyi*) in mice, hamsters, rats and sheep. *Toxicol. Lett.* **56**, 33–41 (1991).
- Andriambeloson, E. et al. Methyllycaconitine- and scopolamine-induced cognitive dysfunction: differential reversal effect by cognition-enhancing drugs. *Pharmacol. Res. Perspec.* **2**, e00048 (2014).
- Stojiljkovic, M. et al. Selective activation of A7 nicotinic acetylcholine receptors augments hippocampal oscillations. *Neuropharmacology* **110**, 102–108 (2016).
- MetaHIT Consortium, Qin, J. et al. A human gut microbial gene catalogue established by metagenomic sequencing. *Nature* **464**, 59–65 (2010).
- Alcalá, J. A. et al. Reversal training facilitates acquisition of new learning in a Morris water maze. *Learn. Behav.* **48**, 208–220 (2020).
- Besheer, J. & Bevins, R. A. The role of environmental familiarization in novel-object preference. *Behav. Process.* **50**, 19–29 (2000).
- Reigstad, C. S. et al. Gut microbes promote colonic serotonin production through an effect of short-chain fatty acids on enterochromaffin cells. *FASEB J.* **29**, 1395–1403 (2015).
- Chen, J. et al. Screening of reliable reference genes for the normalization of RT-qPCR in chicken Gastrointestinal tract. *Poult. Sci.* **102**, 103169 (2023).
- Hellstrom-Lindahl, E. Modulation of b-amyloid precursor protein processing and tau phosphorylation by acetylcholine receptors (2000).
- Khalifeh, S. et al. Beyond the 5-HT₃ receptors: A role for α 7nACh receptors in neuroprotective aspects of Tropisetron. *Hum. Exp. Toxicol.* **34**, 922–931 (2015).
- Bitchi, M. B. et al. Isolation and structure Elucidation of cyclopeptide alkaloids from the leaves of *Heisteria parvifolia*. *Phytochemistry* **167**, 112081 (2019).
- Hall, J., Thomas, K. L. & Everitt, B. J. Rapid and selective induction of BDNF expression in the hippocampus during contextual learning. *Nat. Neurosci.* **3**, 533–535 (2000).
- Mariadason, J. M. et al. Effect of butyrate on paracellular permeability in rat distal colonic mucosa *ex vivo*. *J. Gastro Hepatol.* **14**, 873–879 (1999).
- Spiller, R. & Lam, C. An update on Post-infectious irritable bowel syndrome: role of genetics, immune activation, serotonin and altered Microbiome. *J. Neurogastroenterol Motil.* **18**, 258–268 (2012).
- Cone, R. A. Barrier properties of mucus. *Adv. Drug Deliv. Rev.* **61**, 75–85 (2009).
- Gershon, M. D. Serotonin is a sword and a shield of & the bowel: Serotonin plays offense and defense.
- Boess, F. G. et al. Pharmacological and behavioral profile of N-[(3R)-1-azabicyclo[2.2.2]oct-3-yl]-6-chinolincarboxamide (EVP-5141), a novel A7 nicotinic acetylcholine receptor agonist/serotonin 5-HT₃ receptor antagonist. *Psychopharmacology* **227**, 1–17 (2013).
- Turek, J. W. A sensitive technique for the detection of the α 7 neuronal nicotinic acetylcholine receptor antagonist, Methyllycaconitine, in rat plasma and brain.
- Furuse, M. et al. Occludin: a novel integral membrane protein localizing at tight junctions. *J. Cell Biol.* **123**, 1777–1788 (1993).
- Stevenson, B. R. et al. ZO-1 and cingulin: tight junction proteins with distinct identities and localizations. *Am. J. Physiology-Cell Physiol.* **257**, C621–C628 (1989).
- Wang, R. et al. Four-week administration of nicotine moderately impacts blood metabolic profile and gut microbiota in a diet-dependent manner. *Biomed. Pharmacother.* **115**, 108945 (2019).
- Khailova, L. et al. Bifidobacterium bifidum improves intestinal integrity in a rat model of necrotizing Enterocolitis. *Am. J. Physiology-Gastrointestinal Liver Physiol.* **297**, G940–G949 (2009).
- Mossad, O. et al. Gut microbiota drives age-related oxidative stress and mitochondrial damage in microglia via the metabolite N6-carboxymethyllysine. *Nat. Neurosci.* **25**, 295–305 (2022).

27. Qi, L. et al. Comparative analysis of intestinal microflora between two developmental stages of *rimicaris Kairei*, a hydrothermal shrimp from the central Indian ridge. *Front. Microbiol.* **12**, 802888 (2022).
28. Calder, P. C. & Kew, S. The immune system: a target for functional foods? *Br. J. Nutr.* **88**, S165–S176 (2002).
29. Louis, P. & Flint, H. J. Diversity, metabolism and microbial ecology of butyrate-producing bacteria from the human large intestine. *FEMS Microbiol. Lett.* **294**, 1–8 (2009).
30. Chang, S.-C. et al. A gut butyrate-producing bacterium *Butyrivibrio* regulates short-chain fatty acid transporter and receptor to reduce the progression of 1,2-dimethylhydrazine-associated colorectal cancer. *Oncol Lett* **20**, 327 (2020).
31. Pu, Y. et al. A role of the subdiaphragmatic vagus nerve in depression-like phenotypes in mice after fecal microbiota transplantation from *Chrna7* knock-out mice with depression-like phenotypes. *Brain. Behav. Immun.* **94**, 318–326 (2021).

Author contributions

C.C.: Conceptualization, Methodology, Validation, Data curation, Writing – original draft, Writing –review & editing. S.L.: conceptualization, Methodology, Data curation. W.W.: Conceptualization, Data curation. L.S. and R.M.: Methodology, Software. Qian Deng: Methodology. B.Z.: Funding acquisition. J.T.: Conceptualization, Visualization, Supervision, Project administration, Funding acquisition. All authors commented on previous versions of the manuscript and approved the final manuscript. All authors read and approved the final manuscript.

Funding

This work was supported by the Natural Science Foundation of Ningxia Province (2021AAC03398) and the Ningxia Hui Autonomous Region Key R&D Program (2022BEG03165).

Declarations

Competing interests

The authors declare no competing interests.

Ethical approval

SD rats were purchased from the Laboratory Animal Center of Ningxia Medical University (laboratory animal license No. SCXK (Ning) 2020–0001). The present study in the Animal experiments has been reviewed and approved by the Laboratory Animal Ethical and Welfare Committee of Ningxia Medical University Laboratory Animal Center (ethical code NO. 2018-050).

Additional information

Supplementary Information The online version contains supplementary material available at <https://doi.org/10.1038/s41598-025-02627-2>.

Correspondence and requests for materials should be addressed to B.Z. or J.T.

Reprints and permissions information is available at www.nature.com/reprints.

Publisher's note Springer Nature remains neutral with regard to jurisdictional claims in published maps and institutional affiliations.

Open Access This article is licensed under a Creative Commons Attribution-NonCommercial-NoDerivatives 4.0 International License, which permits any non-commercial use, sharing, distribution and reproduction in any medium or format, as long as you give appropriate credit to the original author(s) and the source, provide a link to the Creative Commons licence, and indicate if you modified the licensed material. You do not have permission under this licence to share adapted material derived from this article or parts of it. The images or other third party material in this article are included in the article's Creative Commons licence, unless indicated otherwise in a credit line to the material. If material is not included in the article's Creative Commons licence and your intended use is not permitted by statutory regulation or exceeds the permitted use, you will need to obtain permission directly from the copyright holder. To view a copy of this licence, visit <http://creativecommons.org/licenses/by-nc-nd/4.0/>.

© The Author(s) 2025